doi:10.14311/ppt.2017.3.281
Plasma Physics and Technology **4**(3):281–285, 2017

MODELING OF THE INTERACTION BETWEEN THE SWITCHING ARC AND HYDRAULIC DRIVING MECHANISM IN GAS-BLAST CIRCUIT BREAKERS

H. Zhang[a], K. Cao[b], Q. Zhang[b], J.D. Yan[b,*]

[a] *Pinggao Group Co. Ltd., Pingdingshan City, Henan, China, 467001*
[b] *Department of Electrical Engineering, University of Liverpool, Brownlow Hill, Liverpool, UK*
[*] yaneee@liverpool.ac.uk

Abstract. The presence of an arc in a circuit breaker interrupter creates an opposing force to the driving mechanism by changing of the pressure field. This opposing force alters the dynamics of the driving mechanism, the travel characteristics of the moving contact and therefore the switching process. The severity of the influence depends on the structure of the interrupter, the travel profile and also the current waveform, especially the magnitude of the fault current. A 252 kV puffer circuit breaker was used in the present work to study the key factors that contribute to the uncertainty of the predicted contact travel based on coupled simulation.

Keywords: Coupled simulation, driving mechanism, switching arc.

1. Introduction

High voltage circuit breaker is a crucial element in modern power transmission system and its reliability and performance play an important role in the safe operation of the network. It is well known that the performance of a breaker is determined by the design and operational parameters among which the travel characteristics of the moving components (e.g. contact-nozzle assembly) is a key factor that is controlled by the driving mechanism but modified by the arcing process. Despite that much effort has been devoted to arc modelling in high voltage circuit breakers [1–3] little has been reported on the influence of the arc on the dynamics of the driving mechanism. Measured travel curves are normally used in the simulation of high voltage circuit breaker [4]. A detailed analysis of a typical three-level hydraulic driving mechanism is given in [5]. As a continuation of the work done in [5], coupled circuit breaker simulation was attemped in [6]. However, the complex arcing process was approximated by a simple pressure device and assumed pressure variation with time. In the present work, a lumped mechanical model of a hydraulic driving mechanisms has been developed and coupled to a differential arc model in a way as shown in figure 1. The coupling between the two models allows the determination of the travel characteristics of the moving components in a self-consistent manner, considering automatically the effect of pressure field variation in the arcing process. The aim is to answer the following two questions. First, using the lumped model for the driving mechanism, what are the main factors that affect the accuracy of the predicted travel characteristics and how? Secondly, what accuracy can be achieved and what is the applicability of the model parameters?

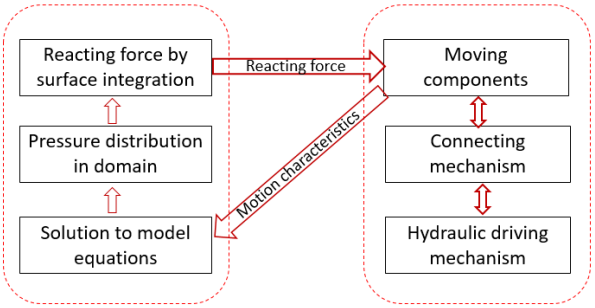

Figure 1. Coupling of the mechanical driving mechanism and the arcing process.

2. Arc model

The gas flow in the interruption chamber is largely unsteady and turbulent with the assumption that the arc is axis-symmetric (2-D). The governing equations (modified Naiver-Stokes equation) of switching arcs can be written in a general form as:

$$\frac{\partial(\rho\phi)}{\partial t} + \nabla\cdot(\rho\phi\vec{V}) - \nabla\cdot(\Gamma_\phi\nabla\psi) = S_\phi \qquad (1)$$

With a comprehensive description of the arc model given in [7, 8], for the sake of simplicity, details regarding the arc model and equation (1) will not be presented in this paper.

The modified N-S equation takes into account all important process and factors during arcing, such as: radiation, ohmic heating, nozzle ablation, electromagnetic effect and turbulence. The arc model is implemented in a commercial computational fluid dynamics (CFD) package, PHOENICS. A typical 252 kV puffer circuit breaker has been chosen as an example, based on which two stes of reference simulation have been conducted with current of 10 and 50 kA.

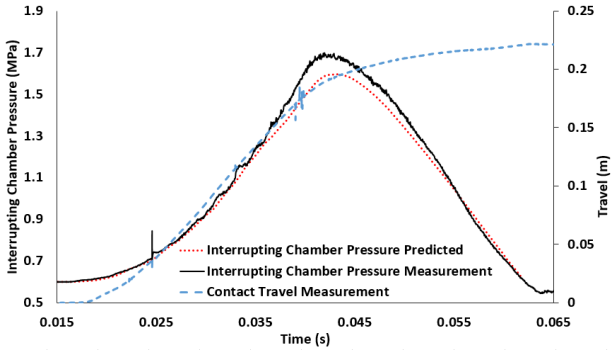

Figure 2. Predicted and measured pressure in the compression chamber of a puffer circuit breaker under 10 kA conditions. Measured contact travel is also given.

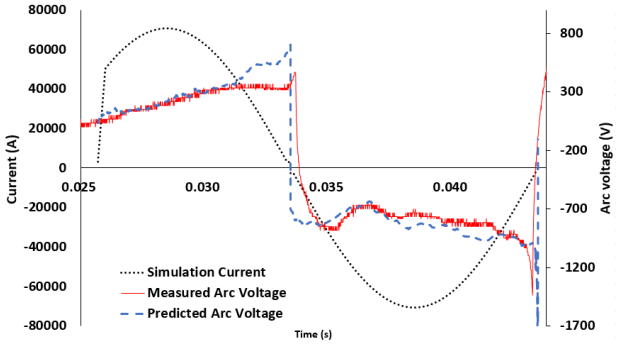

Figure 3. The comparison of simulation and measured arc voltage under 50 kA conditions.

The calculation results are then compared with available measurement. Detailed experimental procedure regarding the measurement of contact travel, arc voltage and interruption chamber pressure is presented in [9]. In the case of 10 kA, a comparison between the measured and simulation arc chamber pressure is provided in figure 2. At 10 kA, the current is relatively low and the arc duration is also short. Thus, the arc has less impact on the pressure distribution in the interruption chamber. As a result, this is an ideal condition to verify pressure predictions caused by compression. On the other hand, at 50 kA, the arc is more stable compared to the low current cases and calculated arc voltage is an important parameter for verifying the arc model. The predicted and measured arc voltage under 50 kA condition are presented in figure 3. The predicted pressure and arc voltage show good agreement with experiment results. The pressure comparison shows that the arc model is capable of predicting the pressure variation in the interruption chamber caused by the moving objects while the arc voltage comparison demonstrates that the arc model is capable of calculating the arc parameters with sufficient accuracy.

3. Hydraulic driving mechanism model

The functional structure of the hydraulic driving mechanism is shown in figure 4. This is a two-level system

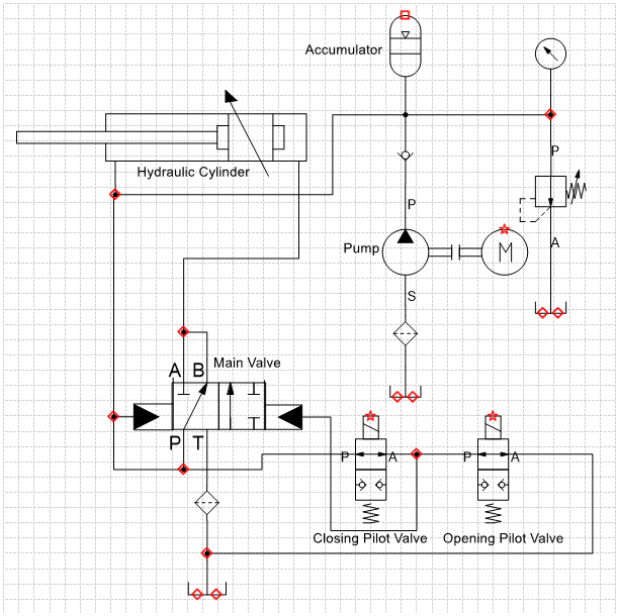

Figure 4. Schematic of the two-level hydraulic driving mechanism upon which the driving mechanism model is based. Only the opening operation is considered. The main components are labled in the diagram.

in the sense that it has two tiers of control valves controlling the operation of the main cylinder i.e. the opening and closing pilot valves and the main valve. The operation of a control valve is a dynamic process, by analyzing the force balance on its control member, this process can be described as:

$$m_i \frac{\mathrm{d}x_i^2}{\mathrm{d}t^2} = F_{\mathrm{s}i} - F_{\mathrm{c}i} - B_{\mathrm{v}i}\frac{\mathrm{d}x_i}{\mathrm{d}t} - F_{\mathrm{r}} \quad i = 1, 2, 3 \quad (2)$$

where the subscript stands for different levels of hydraulic components (1: pilot valve, 2: main valve, 3: hydraulic cylinder), m represents the mass of the control member (mass of the connecting mechanism is included in the hydraulic cylinder level), B_{v} is the viscous friction coefficient, F_{r} the reacting force (only applies to hydraulic cylinder), F_{s} and F_{c} are the forces on the high pressure (system pressure) and control side of the control member, which can be expressed as:

$$F_{\mathrm{s}i} = A_{\mathrm{s}i}P_{\mathrm{s}i} \quad F_{\mathrm{c}i} = A_{\mathrm{c}i}P_{\mathrm{c}i} \quad i = 2, 3$$

where A_{s} and A_{c} are the effective high pressure and control side areas of the control member, P_{s} and P_{c} are the corresponding pressures. Note that the pilot valves are not differential valves, they are operated by electrical actuators. The high-pressure side of any control member can be considered as connected to the accumulator directly since the pressure loss along connecting pipelines is negligible [10]. Therefore, the high-pressure side pressure is equal to the pressure inside the accumulator, which is assumed to remain constant throughout the operation (45 MPa). The pressure of the control side can be calculated using:

Figure 5. Structure of the interruption chamber used in the simulation.

$$\frac{\mathrm{d}P_{ci}}{\mathrm{d}t} = \frac{\beta}{V_{ci}}\left(A_{ci}\frac{\mathrm{d}x_i}{\mathrm{d}t} - Q_{i-1}\right) \quad i = 2,3 \qquad (3)$$

where β is the bulk modulus of the hydraulic oil, V_{ci} the instantaneous volume of the control side chamber and Q_{i-1} is the volumetric flow rate that exits the control side volume. The subscript $_{i-1}$ indicates that the outflow of the current level is always controlled by the previous level component. The flow rate through the control valves is determined by:

$$Q_i = C_{\mathrm{d}i}A_{\mathrm{v}i}\sqrt{\frac{2(P_{\mathrm{c}(i+1)} - P_{\mathrm{b}})}{\rho_{\mathrm{h}}}} \quad i = 1,2 \qquad (4)$$

where C_{d} is the discharge coefficient of the orifice, P_{b} the back pressure (pressure in the oil reservoir, when compared with the operational pressure of the system, it can be considered as atmospheric pressure), ρ_{h} the density of hydraulic fluid and A_{v} the coressponding orifice area. Equations (2)–(4) constitute the governing equations of the hydraulic driving mechanism. By solving them simultaneously, the travel profile of the moving components (without considering reacting force) can be obtained.

4. Reacting force calculation and coupled simulation procedure

The reacting force applied to the driving mechanism is determined by the net force acted by the working gas on the surface of all moving components. This can be obtained by integrating on the surface of all moving components the elementary forces exerted by the pressure in the direction of movement. Within each simulation time step, an integration is performed and the total net reacting force calculated. This new data is then substituted into equation (2) (for hydraulic cylinder only), and a new displacement for the moving components is subsequently obtained. In this manner, the interaction between the arc and the driving mechanism can be included in the predicted travel during the simulation. Structure of the arc chamber under investigation is shown in figure 5. It is a 2-D axis symmetric representation of the actual arc chamber. Filling pressure inside the chamber is 0.6 MPa, the maximum travel of the moving contact (downstream) is 220 mm and the over-travel is 47 mm.

5. Analysis of travel characteristics

During the operation of the hydraulic driving mechanism, the motion of the mechanical components is closely coupled with the flow of hydraulic fluid, such flow is generally complicated since it involves the acceleration, deacceleration, and compression of the fluid. In addition, there are various friction sources that exist between both fluid-solid and solid-solid interfaces. Therefore, it is inevitable that the lumped parameter model contains a number of uncertainties, among which the most prominent is one the frictional force exerted on the piston-rod assembly inside hydraulic cylinder. The magnitude of this frictional force is determined by material, structure of the cylinder as well as the contact area between piston-rod assembly and hydraulic oil. When, a constant $B_{\mathrm{v}3}$ (1250 $\frac{\mathrm{N{\cdot}s}}{\mathrm{m}}$) is used in equation (2) to model the frictional force, the travel curve (for 10 kA case) obtained deviates from the measurement as shown in figure 6. Evidently, a constant $B_{\mathrm{v}3}$ is inadequate. Considering the contact area between the rod and hydraulic oil changes during the motion of the piston, it is necessary to divide $B_{\mathrm{v}3}$ into two parts: a constant part that describes the friction between the piston and the rubber sealing rings installed between the piston and cylinder housing and a linearly changing part that accounts for the changing area of solid-fluid interface i.e.:

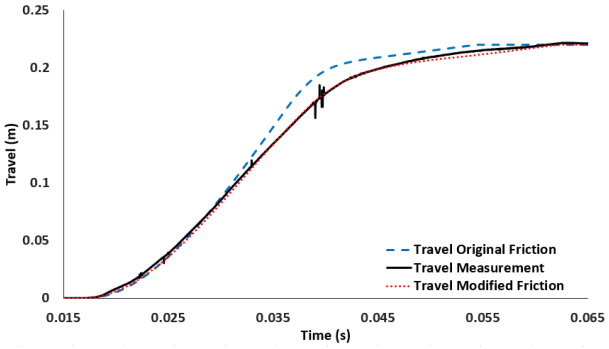

Figure 6. Travel curves for 10 kA case, together with measured travel and travel obtained under same condition with original B_{v3} setup.

$$B_{\mathrm{v}3} = a + b_{x_3} \qquad (5)$$

The value of $B_{\mathrm{v}3}$ is calculated based on experimental results. Figure 6 also presents the travel curve obtained using equation(5). It can be seen that the new result is significantly improvemened over the previous one. The maximum error (1.8%) occurred near the end of the travel is within the acceptable limit. As long as the hydraulic driving mechanism under consideration has a similar structure, the lumped driving mechanism model is capable of predicting the travel profile accurately.

Under high current conditions, another important factor that affects the travel is the reacting force. In this case, the arc can raise the local pressure significantly as shown in figure 7 with both measured and predicted compression chamber pressure. As the moving components are only allowed for translation movement in the arc chamber, their area subjected

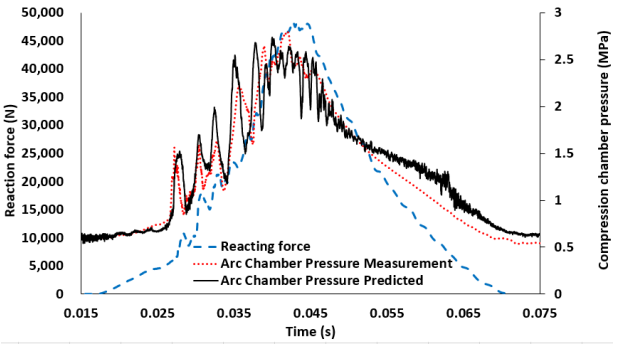

Figure 7. Calculated pressure and reacting force under 50 kA conditions, together with the measured arc chamber pressure. Pressure variations in the figure are recorded at the exit of compression chamber.

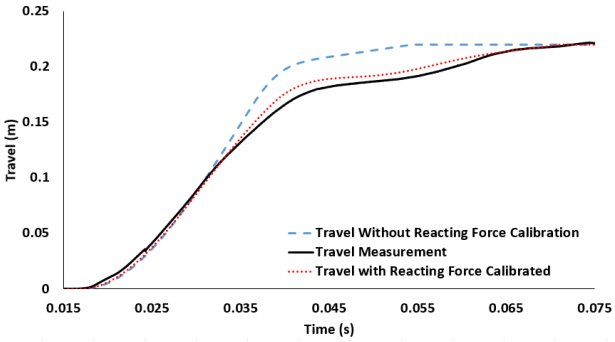

Figure 8. Travel curves for 50 kA case, together with measured travel obtained under same condtion.

to high pressure will remain unchanged throughout the simulation. Thus, the arc will have a much higher impact on the travel compared with the 10 kA case. As showcased in figure 7, although the general profile of the predicted and measured pressure matched up nicely, their instantaneous value still differs. Between 27 ms and 39 ms, the predicted pressure is lower than the measured pressure. As a result, an error naturally exists between the calculated reacting force and its real value. This is further demonstrated by the calculated and measured travel curve as compared in figure 8. It can be observed that a significant difference exists between the two travel profiles. The arc model has underestimated the reacting force as the calculated travel indicates a higher contact speed in the middle portion. To quantify the effect of error in pressure calculation, a dimensionless coefficient is introduced so the total reacting force is:

$$F_\mathrm{r} = B_\mathrm{r} \int P \cdot \mathrm{d}A \tag{6}$$

where F_r is the total reacting force and $\mathrm{d}A$ is the elementary surface area contributing to reacting force that is projected in the direction of movement. B_r is the coefficient used to adjust for the error in pressure calculation, and P is the corresponding local pressure. By comparing with measured travel curve, it is found that the optimum value for B_r is 1.15. The calibrated travel is also shown in figure 8. In this case, the maximum error occurred in the middle portion of the travel profile is 5.8%. It is noteworthy that in the 50 kA case, the maximum reacting force recorded is 47 kN. Considering that the driving mechanism is only capable of outputing 31 kN at most, the reacting force is definitely an important factor when determining the travel profile of the moving components under high current conditions.

6. Conclusion

For no-load and low current cases, the main factor that affects the travel is the frictional force on the cylinder piston. The coefficient for this frictional force should be adjusted using the measured travel as a reference. On the other hand, calculation of pressure distribution in the arc chamber may not always be accurate due to the complex physical processes and geometry. Therefore, the reacting force which essentially quantifies the interaction between the driving mechanism and arcing chamber of a circuit breaker also needs to be calibrated accurately. Despite these uncertainties, the coupled circuit breaker model is capable of describing the operation process under both low and high current conditions. Therefore, it is a valuable tool for circuit breaker design optimization.

References

[1] G. Bizjak, P. Zunko, and D. Povh. Circuit breaker model for digital simulation based on mayr's and cassie's differential arc equations. *IEEE Transactions on Power Delivery*, 10(3):1310–1315, 1995. doi:10.1109/61.400910.

[2] R.E. Blundell and M.T.C. Fang. A simplified turbulent arc model for the current-zero period of a SF_6 gas-blast circuit breaker. *Journal of Physics D: Applied Physics*, 31(5):561–568, 1998. doi:10.1088/0022-3727/31/5/013.

[3] M. Okamoto, M. Ishikawa, K. Suzuki, and H. Ikeda. Computer simulation of phenomena associated with hot gas in puffer-type gas circuit breaker. *IEEE Transactions on Power Delivery*, 6(2):833–839, 1991. doi:10.1109/61.131142.

[4] A. Petchanka, F. Reichert, F. Methling, and S. Franke. CFD arc simulation of a switching-off process in a model chamber. *Plasma Physics and Technology*, 2(1):63–66, 2015. URL: http://ppt.fel.cvut.cz/articles/2015/petchanka.pdf.

[5] B. Xu, R. Ding, J. Zhang, and Q. Su. Modeling and dynamic characteristics analysis on a three-stage fast-response and large-flow directional valve. *Energy conversion and management*, 79:187–199, 2014. doi:10.1016/j.enconman.2013.12.013.

[6] B. Xu, R. Ding, J. Zhang, L. Sha, and M. Cheng. Multiphysics-coupled modeling: Simulation of the hydraulic-operating mechanism for a SF_6 high-voltage circuit breaker. *IEEE/ASME Transactions on Mechatronics*, 21(1):379–393, 2016. doi:10.1109/TMECH.2015.2460351.

[7] K.Y. Park and M.T.C. Fang. Mathematical modeling of SF_6 puffer circuit breakers. I. High current region. *IEEE Transactions on Plasma Science*, 24(2):490–502, 1996. doi:10.1109/27.510015.

[8] K.Y. Park, X.J. Guo, R.E. Blundell, M.T.C. Fang, and Y.J. Shin. Mathematical modeling of SF_6 puffer circuit breakers. II. Current zero region. *IEEE Transactions on Plasma Science*, 25(5):967–973, 1997. doi:10.1109/27.649608.

[9] J.Y. Zhong, Y.J. Guo, and H. Zhang. Pressure and arc voltage measurement in a 252 kV SF_6 puffer circuit breaker. *Plasma Science and Technology*, 18(5):490–493, 2016. doi:10.1088/1009-0630/18/5/08.

[10] H.E. Merritt. *Hydraulic control systems*. John Wiley & Sons, 1967.